arXiv:0805.1751v1 [cond-mat.stat-mech] 13 May 2008

# Universal Long-time Behavior of Nuclear Spin Decays in a Solid

S. W. Morgan,[1,*] B. V. Fine,[2,3] and B. Saam[1,†]

[1] *Department of Physics, University of Utah, 115 South 1400 East, Salt Lake City, Utah 84112-0830, USA*
[2] *Department of Physics and Astronomy, University of Tennessee, Knoxville, TN 37996-1200, USA*
[3] *Institut für Theoretische Physik, Universität Heidelberg, Philosophenweg 19, 69120 Heidelberg, Germany*

(Dated: April 30, 2008)

Magnetic resonance studies of nuclear spins in solids are exceptionally well suited to probe the limits of statistical physics. We report experimental results indicating that isolated macroscopic systems of interacting nuclear spins possess the following fundamental property: spin decays that start from different initial configurations quickly evolve towards the same long-time behavior. This long-time behavior is characterized by the shortest ballistic microscopic timescale of the system and therefore falls outside of the validity range for conventional approximations of statistical physics. We find that the nuclear free induction decay and different solid echoes in hyperpolarized solid xenon all exhibit sinusoidally modulated exponential long-time behavior characterized by identical time constants. This universality was previously predicted on the basis of analogy with resonances in classical chaotic systems.

The relationship between statistical physics and chaos is one of the most important and controversial problems in theoretical physics. Statistical physics is based on the assumption of some kind of randomness on the microscopic scale, yet the question of whether this randomness is at all related to the mathematical concept of chaos (well-established for few-body classical systems) is not well understood [1, 2]. In many-body systems, it is extremely difficult to separate the effects of randomness associated with true chaos from those associated with averaging over the macroscopic number of degrees of freedom [3, 4, 5, 6]. The situation is further complicated by the lack of consensus on the universal definition of chaos in quantum systems. In view of these complications, one approach is to proceed on the basis of conjectured parallels between the properties of mathematical chaotic systems and real many-body systems. The predicted consequences of these conjectures can then be tested numerically or experimentally. One such prediction about the universal long-time behavior of transient nuclear spin decays in solids has been made recently in Ref. [7]. The work presented here tested that prediction by measuring the transverse relaxation of $^{129}$Xe nuclei (spin = 1/2) in solid xenon over four orders of magnitude using nuclear magnetic resonance (NMR). Such experiments are prohibitively challenging for conventional NMR due to the weak thermal magnetization achievable in even the strongest magnets. We have employed the technique of spin-exchange optical pumping [8] in order to achieve enhanced (hyperpolarized) magnetization required for this experiment.

In nearly perfect agreement with the prediction of Ref. [7], our experiments indicate that the long-time behavior of transverse nuclear spin decays in solids has the universal functional form

$$F(t) = A\mathrm{e}^{-\gamma t}\cos(\omega t + \phi), \tag{1}$$

where the decay coefficient $\gamma$ and the beat frequency $\omega$ are *independent of the initially generated transverse spin configuration*. This long-time behavior sets in after only a few times $T_2$, where $T_2$ is the characteristic timescale for transverse decay determined by the interaction between nuclear spins (see Eq. (2) below) and represents the shortest ballistic timescale in the system. The values of $1/\gamma$ and $1/\omega$ are also on the order of $T_2$. Hence, it cannot be that the spins are interacting with a fast-equilibrating heat bath, which would justify the exponential character of the decay, as for a common damped harmonic oscillator. Indeed, at 77 K in an applied magnetic field $\geq 1$ T, the $^{129}$Xe spins are well isolated from their environment. The longitudinal relaxation time $T_1 \approx 2.3$ h [9] while $T_2 \approx 1$ ms [10]; therefore, the decay cannot be attributed to spin-lattice relaxation. The oscillations in this decay, sometimes referred to as Lowe beats [11], constitute a correlation effect [12, 13] induced by the spin-spin interaction and have nothing to do with the Larmor frequency. We verified that the effects of radiation damping and inhomogeneities in the external field are also negligible on the timescale of $T_2$ [14]. The observed decay thus represents the approach of a closed quantum system to equilibrium.

We used the particular pulse sequence (see Fig. 1), known as a solid echo [3, 14], which consists of two 90° pulses (the first along the y-axis and the second along the x-axis in the rotating frame) separated by a delay time $\tau$. In contrast with the conventional Hahn spin echo [16] or the magic echo [17], the solid echo is not an amplitude-attenuated reproduction of the free induction decay (FID) that peaks at time $2\tau$. Complete refocusing by solid echoes occurs only for isolated pairs of spins [3]. A deviation from complete refocusing is caused by higher-order correlations involving more than two spins. The solid echo response depends on the spin configuration just after the second pulse, whereby different values of the delay time $\tau$ imply fundamentally different "after-pulse" configurations [14] that evolve from the uniformly

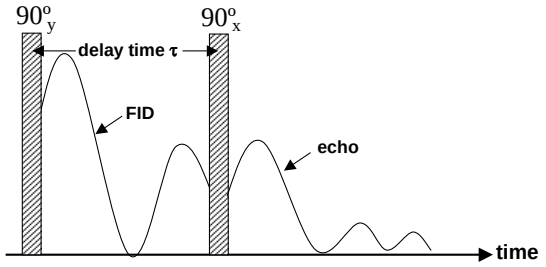


FIG. 1: The pulse sequence used to generate a solid echo. The magnitude of the free-induction decay (FID) including Lowe beats is shown schematically after the first pulse with the solid-echo response shown after the second pulse. The pulses are separated in phase by 90°: the first is along the rotating-frame y-axis, the second is along the rotating-frame x-axis. Unlike conventional Hahn echoes, the solid echo does not generally peak at time $2\tau$[14].

polarized uncorrelated spin state at the beginning of the FID to highly correlated states induced by spin-spin interactions during the delay time [18]. Experimentally, these distinct after-pulse configurations are exactly what is required in order to clearly demonstrate the evolution to a universal long-time behavior.

On the timescale of our experiments, the system of interacting $^{129}$Xe nuclei can be accurately described as isolated and governed by the Hamiltonian of the truncated magnetic dipolar interaction [19, 20], which in the Larmor rotating reference frame has the form

$$\mathcal{H} = \sum_{k<n} [B_{kn}(I_k^x I_n^x + I_k^y I_n^y) + A_{kn} I_k^z I_n^z], \qquad (2)$$

where $A_{kn}$ and $B_{kn}$ are coupling constants and $I_n^i$ are the spin operators representing the $i$th projection of the $n$th spin. The Hamiltonian in Eq. (2) is appropriate in the high-field limit where the Zeeman energy dominates dipolar couplings; hence, the shape and duration of the FID are independent of the applied field. The characteristic decay timescale $T_2$ is on the order of a few inverse nearest-neighbor coupling constants. Although the coupling constants in the Hamiltonian Eq. (2) can be very accurately determined from first principles, efforts over several decades [4, 11, 19, 20, 21, 22, 24, 25] to predict the entire behavior of FIDs and spin echoes quantitatively have met only with limited success; direct calculations tend to lose predictive power in the long-time tail of the decay, where increasingly higher-order spin correlations become important [18]. Although methods have not yet been developed for the controllable calculation of $\omega$ and $\gamma$ in Eq. (1), Ref. [7] predicted the quick onset [12] of the long-time behavior of Eq. (1) with the same values of $\omega$ and $\gamma$ for all kinds of transverse decays in the same system. This prediction was based not on a conventional statistical theory but on a conjecture [12] that quantum spin dynamics generates extreme randomness analogous to classical chaos.

The long-time behavior of Eq. (1) for the FID alone has been previously observed in NMR experiments on $^{19}$F in $CaF_2$ [26]. Analogous observations have also been made in numerical simulations of both classical [27] and quantum [28] spin lattices. Our experiment adds a new insight into this universality by demonstrating that the above long-time behavior is common to both FIDs and solid echoes in the same spin system. Since solid echoes initiated at different delay times $\tau$ start from distinct initial spin configurations, our findings suggest that the tails of transient nuclear spin signals are independent of initial conditions (apart from the oscillation phase and the overall amplitude).

For our experiments, both isotopically natural (26.4% $^{129}$Xe, 21.29% $^{131}$Xe) and enriched (86% $^{129}$Xe, 0.13% $^{131}$Xe) samples of solid polycrystalline xenon containing $^{129}$Xe polarized to 5-10% were prepared using spin-exchange convection cells [1, 14]. FIDs and solid echoes were acquired at 77 K in an applied field of 1.5 T ($^{129}$Xe Larmor frequency of 17.6 MHz), well into the high-field limit of Eq. (2). The enormous dynamic range of these signals required a separate acquisition of the initial and long-time decays for each FID and echo using different gain settings for the NMR receiver [14].

In Fig. 2a, representative decays of the signal magnitude for the FID and solid echoes with three different delay times $\tau$ are shown for enriched xenon on a semilog plot, with the time axis referenced to $\approx 100$ $\mu$s (instrumental dead time) after the end of the first 90° pulse, i.e., at the start of the FID. The FID and each echo are acquired separately with the sample newly polarized, whereby the run-to-run variation in polarization prohibits a direct measurement of their relative amplitudes. Hence, the data for each echo are shown at the proper temporal location, starting $\approx 100$ $\mu$s after the corresponding value of $\tau$, and each echo is normalized to match the FID amplitude at $t = \tau$. Fig. 2b shows the same four acquisitions time-shifted and amplitude-normalized relative to the FID to yield the best overlap at long times ($\approx 2.7$ ms and later after the start of the FID or echo). The decay coefficient $\gamma$ and beat frequency $\omega$ were obtained for each decay from a fit of the long-time signal magnitude to the absolute value of Eq. (1); a representative fit is shown in red. The results are summarized in Table I, where each entry represents the average of fits for six separate acquisitions of the FID or solid echo. For a given isotopic concentration of $^{129}$Xe, the parameters $\gamma$ and $\omega$ are the same for both the FID and all solid echoes independent of the delay time $\tau$.

In contrast, there is no universal behavior in the initial portion of the transverse decays. This is connected to the theoretical expectation (discussed above) that the longer values of the delay time $\tau$ allow higher-order spin correlations that are not refocused by the solid echo to

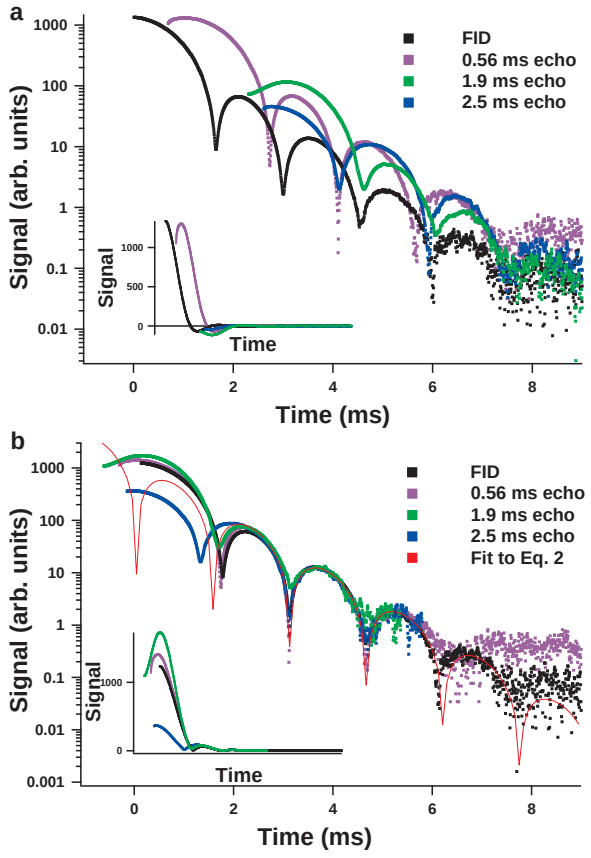


FIG. 2: Representative acquisitions of FID and solid echoes (with three different delay times) recorded for $^{129}$Xe in enriched polycrystalline xenon at 77 K. **a.** The signal magnitudes are shown on a semilog plot (main) and exhibit characteristic beats. The actual signals plotted on a linear scale (inset) change sign, whereas the main plot has cusps at the zero-crossing points. The FID starts at $t = 0$ ms, and each echo starts at its respective delay time $\tau$ with its initial value normalized to the value of the FID at time $\tau$. **b.** The same data are shown again on a semilog plot (main) with the echoes both time- and amplitude-shifted to illustrate the nearly perfect overlap of the long-time decays. For the 1.9 ms and 2.5 ms echoes, the noisiest data farthest out in time have been removed for clarity. The red line is a representative long-time fit to the absolute value of Eq. (1) with the decay coefficient $\gamma = 2.04$ ms$^{-1}$ and the beat frequency $\omega = 1.25$ rad/ms. The distinct differences among the initial portions of the decays can be better appreciated in the linear absolute-value plot (inset).

become stronger. As a result, the initial spin configurations for the FID and various solid echoes are different and not trivially related to one another [14].

In natural xenon, the long-time tails of the FID and the solid echo acquired with delay time $\tau = 0.56$ ms are also nearly identical [14] and can be fit by Eq. (1) with parameters $\gamma$ and $\omega$ given in Table I. The values of both of these parameters are smaller than in the enriched sample because in the natural sample the $^{129}$Xe spins are

| | $\gamma$ (ms$^{-1}$) | $\omega$ (rad/ms) |
|---|---|---|
| Enriched FIDs | $1.25 \pm 0.05$ | $2.03 \pm 0.04$ |
| Enriched echoes, $\tau = 0.56$ ms | $1.25 \pm 0.05$ | $2.00 \pm 0.03$ |
| Enriched echoes, $\tau = 1.9$ ms | $1.22 \pm 0.04$ | $2.06 \pm 0.03$ |
| Enriched echoes, $\tau = 2.5$ ms | $1.25 \pm 0.04$ | $2.05 \pm 0.04$ |
| Natural FIDs | $1.04 \pm 0.08$ | $1.53 \pm 0.08$ |
| Natural echoes, $\tau = 0.56$ ms | $1.04 \pm 0.12$ | $1.52 \pm 0.04$ |

TABLE I: The decay coefficient $\gamma$ and beat frequency $\omega$ extracted from the fit of long-time data by Eq. (1) for FID and solid echo experiments in both natural and $^{129}$Xe-enriched solid xenon. Each entry represents an average of six separate experiments with the errors determined from the spread in the fit results. The delay time $\tau$ is the time between the 90° pulses in the solid echo pulse sequence.

more dilute, having been replaced with zero-spin species or with $^{131}$Xe, for which the dipolar interaction has different coupling constants. The intrinsically weaker signal meant that the long-time tails of echoes with delay times $\tau \gtrsim 0.56$ ms could not be accurately measured.

The common quantitative long-time character of FIDs and spin echoes provides experimental support for the notion of eigenmodes of the time evolution operator $\hat{T}(t)$ in isolated many-body quantum systems. This operator is defined by the equation $\varrho(t, \mathbf{x}) = \hat{T}(t)\varrho(0, \mathbf{x})$, where $\varrho(0, \mathbf{x})$ is the many-body density matrix at some initial time $t = 0$, and $\mathbf{x}$ is the set of variables that describe the density matrix. It was conjectured [7, 12] that in the observable long-time range, the non-equilibrium behavior of the density matrix for any small but macroscopic subsystem of the closed system is controlled by a complex-valued eigenmode having the form:

$$\varrho_0(\mathbf{x})\mathrm{e}^{(-\gamma+i\omega)t} + \varrho_0^*(\mathbf{x})\mathrm{e}^{(-\gamma-i\omega)t}. \qquad (3)$$

If this conjecture is valid, then the long-time decay of Eq. (1) represents not just the property of one relaxation process, such as the FID, but rather an intrinsic property of the many-body dynamics of the system, and should manifest itself in numerous other relaxation processes, such as solid echoes with different delay times $\tau$.

The eigenmodes of the time evolution operator as defined by Eq. (3) have no direct relation to the eigenvalues of the Hamiltonian of the many-body system, but rather they are expected to be counterparts of the Pollicott-Ruelle resonances [1, 30] in classical hyperbolic chaotic systems. These resonances depend on the rate of probability loss from coarser to finer partitions of phase space [1, 2]. In many-body quantum systems, there should exist an analogous transfer of spectral weight from lower to higher order quantum correlations [18].

Quantum analogs of Pollicott-Ruelle resonances have been observed numerically in kicked spin-1/2 chains [31], the kicked quantum top [32], Loschmidt echoes [33], and experimentally for the imitation of the single particle quantum problem in microwave billiards [34]. In all these

cases, the quantum systems had one or several of the following features: (i) very few degrees of freedom; (ii) proximity to the classically chaotic limit; (iii) application of external time-dependent forces, removing the difficulty associated with the discrete frequency spectrum of an isolated quantum system. In contrast, we deal here with an essentially isolated system having a macroscopic number of maximally non-classical components (spins 1/2), and have no specially introduced precondition for chaos apart from the naturally occurring non-integrable interaction between spins.

We note a remarkable fact revealed by Fig. 2a: the phases of the long-time oscillations of the 1.9 ms and 2.5 ms echoes nearly coincide with each other and are shifted by $\pi$ with respect to the FID phase. Indeed, one can observe that the zero-crossings (cusps) of the FID and the two echoes coincide in the long-time regime. Given that these are the absolute-value plots, the above coincidences imply that the relative phases of the long-time signals are either zero or $\pi$. These two possibilities can be discriminated by keeping track of the successive sign changes at the zero-crossings for each signal. (The inset of Fig. 2a shows the sign of the FID and each echo.) This may be a fundamental phase relation associated with the fact that the 1.9 ms and 2.5 ms echoes start after the FID has begun to approach the asymptotic regime of Eq. (1). In contrast, the 0.56 ms echo starts well before the FID has reached that regime, and its phase has no particular relation to the other three signals.

We have observed a universal long-time behavior of $^{129}$Xe FIDs and solid echoes in solid xenon. In all cases, a sinusoidally modulated exponential decay sets in after just a few times $T_2$. This behavior is universal in the sense that the two parameters characterizing the long-time decay are independent of the NMR pulse/delay sequence, even though each such sequence generates a different initial spin configuration. These findings reveal a fundamental property of nuclear spin dynamics. In addition, they also support the idea that the correspondence between classical and quantum chaotic properties of real many-body systems can be established at the level of Pollicott-Ruelle resonances. Further investigations, however, are required in order to clarify whether the eigenmodes of form (3) actually exist in many-spin density matrices and, if so, how far this correspondence can be taken.

The authors are grateful to M. S. Conradi, T. Egami, K. A. Lokshin, and O. A. Starykh for helpful discussions. This work was supported by the National Science Foundation (PHY-0134980).

* Present address: Department of Physics, Princeton University, Princeton, NJ 08544, USA
† Electronic address: saam@physics.utah.edu

[1] P. Gaspard, *Chaos, Scattering and Statistical Mechanics* (Cambridge University Press, Cambridge, 1998).
[2] F. Haake, *Quantum Signatures of Chaos* (Springer-Verlag, Berlin, Germany, 2001).
[3] P. Gaspard, M. E. Briggs, M. K. Francis, J. Sengers, R. W. Gammon, J. R Dorfman, and R. V. Calabrese, Nature **394**, 865 (1998).
[4] C. P. Dettmann, E. G. D. Cohen, and H. van Beijeren, Nature **401**, 875 (1999).
[5] P. Grassberger and T. Schreiber, Nature **401**, 875 (1999).
[6] P. Gaspard, M. E. Briggs, M. K. Francis, J. Sengers, R. W. Gammon, J. R Dorfman and R. V. Calabrese, Nature **401**, 876 (1999).
[7] B. V. Fine, Phys. Rev. Lett. **94**, 247601 (2005).
[8] T. G. Walker and W. Happer, Rev. Mod. Phys. **69**, 629 (1997).
[9] M. Gatzke, G. D. Cates, B. Driehuys, D. Fox, W. Happer, and B. Saam, Phys. Rev. Lett. **70**, 690 (1993).
[10] W. M. Yen and R. E. Norberg, Phys. Rev. **131**, 269 (1963).
[11] I. J. Lowe and R. E. Norberg, Phys. Rev. **107**, 46 (1957).
[12] B. V. Fine, Int. J. Mod. Phys. B **18**, 1119 (2004).
[13] B. V. Fine, Phys. Rev. Lett. **79**, 4673 (1997).
[14] See Supporting Material at the end of this paper for detailed experimental methods, a theoretical description of solid echoes, and natural xenon data.
[3] J. G. Powles and P. Mansfield, Phys. Lett. **2**, 58 (1962).
[16] E. L. Hahn, Phys. Rev. **80**, 580 (1950).
[17] W. K. Rhim, A. Pines and J. S. Waugh, Phys. Rev. B **3**, 684 (1971).
[18] H. Cho, T. D. Ladd, J. Baugh, D. G. Cory and C. Ramanathan, Phys. Rev. B **72**, 054427 (2005).
[19] C. P. Slichter, *Principles of Magnetic Resonance* (Springer-Verlag, New York, NY, 1996 corr. ed.).
[20] A. Abragam, *Principles of Nuclear Magnetism* (Oxford Science Publications, New York, NY, 1961).
[21] J. H. Van Vleck, Phys. Rev. **74**, 1168 (1948).
[22] J. R. Klauder and P. W. Anderson, Phys.Rev. **125**, 912 (1962).
[4] J. G. Powles and J. H. Strange, Proc. Phys. Soc. **82**, 6 (1963).
[24] P. Borckmans and D. Walgraef, Phys. Rev. **167**, 282-288 (1968).
[25] B. Cowan, *Nuclear Magnetic Resonance and Relaxation* (Cambridge University Press, Cambridge, 1997).
[26] M. Engelsberg and I. J. Lowe, Phys. Rev. B **10**, 822 (1974).
[27] B. V. Fine, J. Stat. Phys. **112**, 319 (2003).
[28] K. Fabricius, U. Löw and J. Stolze, Phys. Rev. B **55**, 5833 (1997).
[1] T. Su, G. L. Samuelson, S. W. Morgan, G. Laicher and B. Saam, Appl. Phys. Lett. **85**, 2429 (2004).
[30] D. Ruelle, Phys. Rev. Lett. **56**, 405 (1986).
[31] T. Prosen, J. Phys. A **35**, L737 (2002).
[32] C. Manderfeld, J. Weber and F. Haake, J. Phys. A **34**, 9893 (2001).
[33] G. Benenti, G. Casati, and G. Veble, Phys. Rev. E **67**, 055202(R) (2003).

[34] K. Pance, W. Lu, and S. Sridhar, Phys. Rev. Lett. **85**, 2737 (2000).

## SUPPORTING MATERIAL

(with a separate system of references)

### Detailed Experimental Methods

The samples of solid polycrystalline hyperpolarized $^{129}$Xe were prepared using spin-exchange convection cells [1]. These cells allow the production of large quantities of hyperpolarized $^{129}$Xe by keeping most of the xenon in the liquid phase. The xenon gas is polarized at 100 °C and travels by convection to the column of liquid that is kept cold (−110 °C) in a retort that is open to the rest of the cell. The liquid $^{129}$Xe is polarized by passive phase exchange with the gas. Using these 10 cm$^3$ cells, we have generated a nuclear spin polarization of 5-10% in one liquid sample of 0.7 mM enriched xenon (86% $^{129}$Xe, 0.13% $^{131}$Xe ) and two liquid samples of 2.6 mM natural xenon (26.4% $^{129}$Xe, 21.29% $^{131}$Xe) inside a 1.5 T horizontal-bore superconducting magnet ($^{129}$Xe Larmor frequency of 17.6 MHz).

To study the NMR signals in the solid state, the liquid hyperpolarized xenon was subsequently frozen and maintained at 77 K while still inside the magnet by forcing liquid nitrogen directly into the chamber containing the cell. At 1.5 T, the polarization is expected to survive this phase transition intact [2], and this was verified experimentally by monitoring the NMR signal height with small-angle pulses during freezing. Since 90° rf excitation pulses (pulse length ≈ 10 $\mu$s) are used to obtain the FIDs and solid echoes, the magnetization was essentially destroyed by each acquisition. However, the convection cells allow easy *in situ* regeneration of the $^{129}$Xe polarization, and the experiment could thus be repeated many times per day. The NMR flip angle was calibrated for each separate measurement by applying several identical excitation pulses ($\theta \approx 40°$) and measuring the corresponding $\cos\theta$ magnetization loss. The separate acquisitions of the initial and long-time portions of the decays for each FID and echo were joined together at one point common to both signals and amplitude-renormalized. (The renormalization is necessary because the $^{129}$Xe polarization obtained by spin-exchange optical pumping varies somewhat from run to run.) In one case (the 0.56 ms delay time in enriched Xe), three separate signals had to be acquired, and these were similarly joined together at two locations.

We have examined the possible effects of radiation damping and inhomogeneity in the external field on the FID and solid echo line shapes. The observed transverse decay time $T_2^*$ for hyperpolarized liquid xenon (having approximately the same polarization as the solid) is ≈ 23 ms in the same NMR probe and location in the magnet. (Here, $T_2^*$ refers to the timescale for transverse decay from all sources of dephasing combined.) Unlike the solid case, the spin-spin interactions in the motionally narrowed liquid are much weaker, allowing the decay to be essentially limited by some combination of radiation damping and field inhomogeneity. (Since we observe the liquid lineshape to be independent of polarization, it is likely that field inhomogeneity is actually the limiting factor.) Since the liquid decay is much longer than the ≈ 1 ms decay time observed for the solid, we conclude that the effects of these other sources of dephasing are negligible in the solid. As an additional check, we note that the decay shapes associated with both the field inhomogeneity and the radiation damping are expected to be non-exponential; if these factors were not negligible in our experiments, then the long-time decay of the beat amplitude would exhibit a noticeable departure from an exponential shape.

### Theoretical facts about solid echoes

Solid echoes are produced by the radio frequency pulse sequence $90^\circ_y$−time delay $\tau$−$90^\circ_x$. Here and below all axes are defined in the Larmor rotating reference frame. The pulses are assumed to rotate the spin system instantaneously.

Before the first pulse, the spin system is characterized by the equilibrium density matrix

$$\rho_{\rm eq} = C_N \exp\left\{\frac{M_z H}{k_B T}\right\}, \tag{A.4}$$

where $M_z = g\sum_k I_k^z$ is the total magnetization of nuclei with gyromagnetic ratio $g$ in external magnetic field $H$ directed along the $z$-axis, $k_B$ is Boltzmann's constant, $T$ the temperature (in our case, it is the effective spin temperature of the hyperpolarized system), and $C_N$ is the normalization constant. The usual energy hierarchy $k_BT \gg \hbar g H \gg \hbar/T_2$ is satisfied in our experiment.

The operator of the first $(90^\circ_y)$ pulse is

$$P_1 = \exp\left\{-i\frac{\pi}{2}\sum_k I_k^y\right\}. \tag{A.5}$$

This operator transforms $I_k^z \to P_1^+ I_k^z P_1 = I_k^x$, and, therefore, just after the pulse

$$\rho(0) = P_1^+\rho_{\rm eq}P_1 = C_N\exp\left\{\frac{M_x H}{k_B T}\right\} \approx C_N\left(\mathbb{1} + \frac{M_x H}{k_B T}\right), \tag{A.6}$$

where $M_x = g\sum_k I_k^x$.

Following the first pulse, the system undergoes free induction decay (FID) described as follows:

$$\begin{aligned} F_{\rm FID}(t) \;&\cong \langle M_x(t)\rangle = {\rm Tr}\left\{\textstyle\sum_k I_k^x\, e^{i\mathcal{H}\,t}\,\rho(0)\,e^{-i\mathcal{H}\,t}\right\} \\ &\cong {\rm Tr}\left\{\textstyle\sum_k I_k^x\, e^{i\mathcal{H}\,t}\,\sum_n I_k^n\, e^{-i\mathcal{H}\,t}\right\}, \end{aligned} \tag{A.7}$$

where the second sign $\cong$ implies that we expanded $\rho(0)$ according to Eq.(A.6), dropped the term containing $\mathbb{1}$ as it makes no contribution to the trace, and then omitted the prefactor $\frac{C_N g^2}{k_B T}$. The Hamiltonian $\mathcal{H}$ is given by Eq.(2) of the main article.

The second $(90^\circ_x)$ pulse is characterized by operator

$$P_2 = \exp\left\{-i\frac{\pi}{2}\sum_k I_k^x\right\}. \tag{A.8}$$

The action of this operator is the following:

$$\begin{array}{lll} I_k^x \to & P_2^+ I_k^x P_2 & = I_k^x \\ I_k^y \to & P_2^+ I_k^y P_2 & = -I_k^z \\ I_k^z \to & P_2^+ I_k^z P_2 & = I_k^y \end{array} \tag{A.9}$$

The density matrix just before the second pulse is

$$\rho_-(\tau) = e^{i\mathcal{H}\tau}\,\rho(0)\,e^{-i\mathcal{H}\tau}. \tag{A.10}$$

Just after the pulse, it becomes

$$\rho_+(\tau) = P_2^+\, e^{i\mathcal{H}\tau}\,\rho(0)\,e^{-i\mathcal{H}\tau}\,P_2. \tag{A.11}$$

The action of $P_2^+ ... P_2$ in Eq.(A.11) can be represented as the change of the identity of $I_k^\alpha$ operators according to rules (A.9). (Here $\alpha = x, y, z$.) Indeed, since $P_2 P_2^+ = \mathbb{1}$, any term of the form $P_2^+ I_k^\alpha I_l^\beta ... I_n^\delta P_2$ arising in the expansion of the right-hand-side of Eq.(A.11) is equal to $P_2^+ I_k^\alpha P_2 P_2^+ I_l^\beta P_2 P_2^+ ... P_2 P_2^+ I_n^\delta P_2$, and hence each operator $I_k^\alpha$ is being "rotated" individually. Using the above fact, Eq.(A.11) can be rewritten as

$$\rho_+(\tau) = e^{i\mathcal{H}_{\rm R}\,\tau}\,\rho(0)\,e^{-i\mathcal{H}_{\rm R}\,\tau}, \tag{A.12}$$

where

$$\mathcal{H}_{\rm R} = \sum_{k<n} B_{kn} I_k^x I_n^x \,+\, A_{kn} I_k^y I_n^y \,+\, B_{kn} I_k^z I_n^z. \tag{A.13}$$

(The subscript "R" stands for "Rotated".)

The density matrix at time $t'$ after the second pulse is

$$\rho_{\rm SE}(\tau, t') = e^{i\mathcal{H}\,t'}\,\rho_+(\tau)\,e^{-i\mathcal{H}\,t'}. \tag{A.14}$$

Finally, the solid echo signal is given by

$$F_{\rm SE}(\tau, t') \cong {\rm Tr}\left\{\sum_k I_k^x \;\; e^{i\mathcal{H}\,t'}\, e^{i\mathcal{H}_{\rm R}\,\tau} \sum_n I_k^n \, e^{-i\mathcal{H}_{\rm R}\,\tau}\, e^{-i\mathcal{H}\,t'}\right\}. \tag{A.15}$$

As mentioned in the main article, different delay times $\tau$ imply fundamentally different initial spin configurations, $\rho_+(\tau)$, for the solid echo response. At small $\tau$, $\rho_+(\tau)$ is not much different from $\rho(0)$ given by Eq.(A.6), which describes uncorrelated uniformly polarized spin distribution. As $\tau$ increases, the density matrix $\rho_+(\tau)$ is gradually overtaken by increasingly higher order spin correlations induced by the Hamiltonian $\mathcal{H}_{\rm R}$. This can be seen from the expansion

$$\begin{aligned}\rho_+(\tau) = \;& \rho(0) + i\tau[\mathcal{H}_{\rm R}, \textstyle\sum_k I_k^x] - \frac{\tau^2}{2!}[\mathcal{H}_{\rm R}, [\mathcal{H}_{\rm R}, \textstyle\sum_k I_k^x]] \\ & - \frac{i\tau^3}{3!}[\mathcal{H}_{\rm R}, [\mathcal{H}_{\rm R}, [\mathcal{H}_{\rm R}, \textstyle\sum_k I_k^x]]] + ... \;\; . \end{aligned} \tag{A.16}$$

Each commutation with $\mathcal{H}_{\rm R}$ entails an extra power of operators $I_k^\alpha$. The resulting higher order spin correlations dominate in $\rho_+(\tau)$ at $\tau \gtrsim T_2$. We further note that in this regime, the initial spin configurations for a solid echoes with different delay times $\tau$ are not equivalent to each other.

The correlations induced by $\mathcal{H}_{\rm R}$ are non-trivially connected with those intrinsic for $\mathcal{H}$, the actual Hamiltonian of the system. One can achieve a limited simplification of the problem by expressing $\mathcal{H}_{\rm R}$ as

$$\mathcal{H}_{\rm R} = -\mathcal{H} + \Delta\mathcal{H}, \tag{A.17}$$

where

$$\Delta\mathcal{H} = \sum_{k<n} 2B_{kn} I_k^x I_n^x \,+\, (A_{kn} + B_{kn})(I_k^y I_n^y \,+\, I_k^z I_n^z). \tag{A.18}$$

The advantage of this representation is that $\Delta\mathcal{H}$ commutes with $\sum_k I_k^x$. If it also commuted with $\mathcal{H}$, then the exponent $e^{i(-\mathcal{H}+\Delta\mathcal{H})\,\tau}$ would factorize into $e^{-i\mathcal{H}\,\tau}\, e^{i\Delta\mathcal{H}\,\tau}$, and then $e^{i\Delta\mathcal{H}\,\tau}$ would not influence $\rho_+(\tau)$, while $e^{-i\mathcal{H}\,\tau}$ would lead to a time-reversed evolution and imply the full recovery of the initial state at $t' = \tau$ [i.e. $\rho_{\rm SE}(\tau, \tau) = \rho(0)$].

As mentioned in the main article, such a situation is, indeed, realized for a pair of interacting spins 1/2. In this case, $[\mathcal{H}, \Delta\mathcal{H}] = 0$, because $[I_1^\alpha I_2^\alpha,\; I_1^\beta I_2^\beta] = 0$ for any $\alpha$ and $\beta$. However, for a lattice of spins 1/2, $[\mathcal{H}, \Delta\mathcal{H}] \neq 0$, because the commutators like $[I_1^\alpha I_2^\alpha,\; I_2^\beta I_3^\beta]$ are not equal to zero for $\alpha \neq \beta$.

One can nevertheless conclude that solid echo tends to undo two-spin correlations in many-spin systems. Therefore, at sufficiently small $\tau$, when $\rho_+(\tau)$ is controlled by the first three terms in expansion (A.16), the solid echo can be described as an imperfect attempt at time reversal. (Note that even for small delay time 0.56 ms, the maximum of the solid echo in Fig. 2a of the main article occurs noticeably earlier than at $t = 2\tau$.) When $\tau \gtrsim T_2$, the rigorous calculation of solid echoes becomes intractable, but otherwise it is clear the concept of time reversal becomes increasingly inappropriate.

For further reading, see the original references concerning solid echoes [3, 4].

## Natural Xenon Data

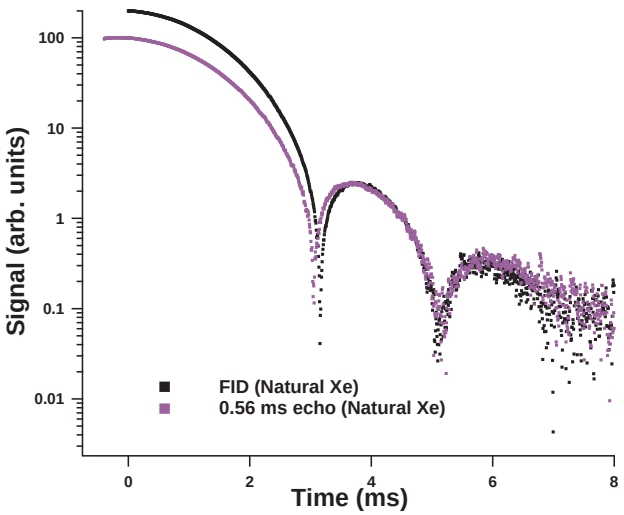


FIG. S1: Representative acquisitions of FID and the 0.56 ms solid echo recorded for $^{129}$Xe in polycrystalline xenon with natural abundance of nuclear isotopes at 77 K. Here, the FID and echo and normalized and time-shifted in the same manner as for enriched xenon in Fig. 2b (main manuscript) to show the overlap in the long-time regime. The long-time behavior of the FID and solid echo are identical in form, although the decay coefficient $\gamma$ and beat frequency $\omega$ each have values smaller than those for enriched xenon; see Table I of main manuscript.

* Present address: Department of Physics, Princeton University, Princeton, NJ 08544, USA
† Electronic address: saam@physics.utah.edu

[1] T. Su, G. L. Samuelson, S. W. Morgan, G. Laicher, and B. Saam, Appl. Phys. Lett. **85**, 2429 (2004).
[2] N. N. Kuzma, B. Patton, K. Raman, and W. Happer, Phys. Rev. Lett. **88**, 147602 (2002).
[3] J. G. Powles and P. Mansfield, Phys. Lett. **2**, 58 (1962).
[4] J. G. Powles and J. H. Strange, Proc. Phys. Soc. **82**, 6 (1963).